


Optical coherence tomography angiography in patients with retinitis pigmentosa who have normal visual acuity

Seiji Takagi,^{1,2,3}  Yasuhiko Hirami,^{1,2,4} Masayo Takahashi,^{1,2,4} Masashi Fujihara,^{1,2} Michiko Mandai,^{1,4} Chisato Miyakoshi,⁵ Goji Tomita³ and Yasuo Kurimoto^{1,2,4}

¹Department of Ophthalmology, Kobe City Medical Center General Hospital, Kobe, Japan

²Department of Translational Research, Division of Ophthalmology, Institute of Biomedical Research and Innovation, Kobe, Japan

³Department of Ophthalmology, Toho University Ohashi Medical Center, Tokyo, Japan

⁴RIKEN Center for Developmental Biology, Kobe, Japan

⁵Department of Pediatrics, Kobe City Medical Center General Hospital, Kobe, Japan

ABSTRACT.

Purpose: To investigate flow area changes measured using optical coherence tomography angiography (OCTA; RTVue XR Avanti[®]) in patients with retinitis pigmentosa (RP) with preserved visual acuity (VA).

Methods: This was an age- and refraction-matched case-control study. Consecutive patients with a best-corrected visual acuity (BCVA) of $\geq 20/20$ and normal subjects were recruited. Fifty eyes (32 patients) and 22 eyes (12 controls) were included. The flow area and foveal avascular zone (FAZ) were measured in both superficial and deep layers within a 3×3 mm central area of the fovea. Association between OCTA parameters and the length of the inner segment ellipsoid (ISE) and external limiting membrane (ELM), the area without abnormal fluorescence in fundus autofluorescence (normal FAF area ratio) and the area of I-2e of the Goldmann perimeter were analysed using mixed-effects regression analysis.

Results: Foveal avascular zones were significantly smaller in patients with RP than in controls in superficial ($p = 0.004$) but not in deep layers ($p = 0.25$). The flow area in superficial ($p = 0.007$) and deep layers ($p = 0.004$) was significantly smaller in patients with RP than in controls. In patients with RP, flow areas in the superficial layers, but not in the deep layers, were significantly associated with the lengths of ISE ($p = 0.001$) and ELM ($p = 0.002$) and the I-2e area ($p = 0.036$), but not with the normal FAF area ratio ($p = 0.399$).

Conclusion: Optical coherence tomography angiography (OCTA)-measured flow area in superficial layers gradually reduced with RP progression and may be a useful parameter of RP pathogenesis.

Key words: coefficient correlation – inner segment ellipsoid – optical coherence tomography angiography – retinitis pigmentosa

Acta Ophthalmol. 2018; 96: e636–e642

© 2018 The Authors. Acta Ophthalmologica published by John Wiley & Sons Ltd on behalf of Acta Ophthalmologica Scandinavica Foundation

This is an open access article under the terms of the Creative Commons Attribution-NonCommercial-NoDerivs License, which permits use and distribution in any medium, provided the original work is properly cited, the use is non-commercial and no modifications or adaptations are made.

doi: 10.1111/aos.13680

Introduction

Retinitis pigmentosa (RP) is the most common form of inherited retinal dystrophy characterized by the progressive impairment and death of retinal photoreceptors (Berson 1993; Hartong et al. 2006). Previous studies have identified mutations in at least 45 genes encoding components of the phototransduction cascade, including proteins involved in retinol metabolism, cell-cell interactions, photoreceptor structural proteins and other splicing factors (den Hollander et al. 2010; Daiger et al. 2013). Retinitis pigmentosa (RP) has a worldwide frequency of 1 in 4000 and is a major cause of inherited blindness or visual handicap in the developed world (Daiger et al. 2013). Clinical studies have revealed that visual field loss starts from the mid-peripheral region in the early stage, with a gradual loss of the peripheral visual field, and the development of tunnel vision due to progressive degeneration of rod and cone photoreceptors. The final impaired central vision is due mainly to cone dystrophy. However, the speed of onset and extent of the disorders are variable, and the pathogenesis has not been fully elucidated.

Because attenuation of retinal vessels is a characteristic finding of RP (Berson 1993; Hartong et al. 2006), circulatory disorders are thought to

play an important role in RP progression. Histopathological studies have revealed that the retinal venules are surrounded by deposits of extracellular matrix, which narrow the vessel lumina of the retinal vasculature (Li et al. 1985). Vessel attenuation is thought predominantly to reflect the reduced metabolic demand of the degenerated retina, where loss of oxygen consumption leads to an increase in local oxygen levels in the retina, ultimately resulting in vasoconstriction (Yu & Cringle 2005; Ma et al. 2012). Clinical reports using various procedures support these findings, including measurements of subfoveal blood flow assessed using laser Doppler flowmetry (Grunwald et al. 1996), and blood flow measurements assessed using laser speckle flowgraphy, both demonstrating a significant reduction in patients with RP (Murakami et al. 2015). Moreover, recently, retinal arterial and venous narrowing at an early stage has been reported by means of a dynamic and static vessel analyser (Iacono et al. 2017).

Optical coherence tomography angiography (OCTA) is a novel, non-invasive imaging technique that is able to construct a map of blood flow in some retinal layers in a few seconds to compare decorrelation signals between sequential OCT B-scans taken at precisely the same cross-section (Jia et al. 2012). Previous cross-sectional OCTA studies showed that the superficial and deep capillary plexus densities are decreased in both early- and late-stage RP (Toto et al. 2016; Parodi et al. 2017).

However, it is yet unclear how these microcirculatory changes correlate with morphological and functional changes. The aim of this study was to investigate the retinal circulation of patients with RP using OCTA to determine whether the OCTA-imaged flow areas were reduced in patients with RP with good VA ($\geq 20/20$), and whether the flow areas correlated with OCT, fundus autofluorescence (FAF) and Goldmann perimeter results.

Patients and Methods

The Kobe City Medical Center General Hospital ethics committee reviewed and approved the protocol for this age- and refraction-matched case-control study and waived the requirement

for informed consent. This study conformed to the tenets of the Declaration of Helsinki.

Patients

Consecutive cases of patients with RP who had BCVA of 20/20 or better were recruited from August 2015 to February 2016 and admitted to the outpatient clinic of Kobe City Medical Center General Hospital. Age- and refraction-matched control subjects were enrolled by colleagues at our hospital. All subjects were Asian. Patients were diagnosed with RP based on clinical history, appearance of the fundus, visual fields and full-field electroretinogram results. At initial visit after the enrolment, all patients had undergone complete ocular examinations including BCVA, slit-lamp biomicroscopy, dilated funduscopy, fundus autofluorescence, OCT and OCTA. BCVA was obtained using Landolt C charts. These values were then converted to the logarithm of the minimum angle of resolution (logMAR) equivalent for statistical comparisons. Exclusion criteria were poor OCTA image quality (described in the next paragraph), refractive errors less than -6 dioptres and greater than $+3$ dioptres, and other potentially confounding retinal pathologies. Patients with cystoid macular oedema, posterior subcapsular cataract or epiretinal membrane were also excluded. The genetic characterization and mode of inheritance were not studied.

Optical coherence tomography angiography (OCTA)

The images were taken within $3 \text{ mm} \times 3 \text{ mm}$ scans centred on the fovea with an RTVue XR Avanti[®] instrument (Optovue[®] Inc., Fremont, CA, USA), which uses a split-spectrum amplitude-decorrelation angiography algorithm to compare decorrelation signals between sequential OCT B-scans taken at precisely the same cross-sections (Version: 2016.100.0.45). Mydriasis was obtained by topical mixed instillation of 0.5% of tropicamide and 10% of phenylephrine before inspection.

The patient was instructed to focus the internal fixation onto the scanning domain. Retina OCT images were

optimized by selecting the Auto All function, including the Auto Z function to decide the appropriate position of the retina and the refraction focus; Auto F function to find the appropriate focus for the patients' refraction; and Auto P function to find the best polarization for the patients' polarization.

Furthermore, the software program carried out a correction technique to remove saccade and fixed light loss. The device obtains volumetric scans of 304×304 A-scans at 70 000 A-scans per second in approximately 3.0 seconds. To obtain the segmentation of these full-thickness retinal scans into the 'superficial', 'deep' and 'choriocapillaris' vascular plexuses, each layer of the alignment was corrected manually. The definition is as described below, with the superficial layer from the inner limiting membrane to the outer limits of the inner plexiform layer, the deep layer from the outer limits of the inner plexiform layer to the outer limits of the inner nuclear layers (INL) and the choriocapillaris from the retinal pigment epithelium (RPE) line to $28 \mu\text{m}$ below the line. FAZ was outlined by manual determinations in the superficial and deep layers. The retinal flow area and FAZ in each layer were binarized and then measured using the internal software of the instrument (Fig. 1A–C).

Reproducibility of two examinations and the intraclass correlation coefficient of the flow area in the OCTA were examined in normal subjects within a 3-month period. OCTA showed increased potential for artefacts of blinks or eye movement, resulting in vessel ghosting. We therefore excluded the poor images that could not be clearly identified at the edge of the vascular wall in retinal veins. We conducted a review of consecutive patients seen by two physicians (S.T, Y.H) individually and the averages; the mean value was used for analysis.

Spectral-domain optical coherence tomography (SD-OCT)

Spectral-domain optical coherence tomography (SD-OCT) images were acquired with an 870-nm light source by the Spectralis[®] HRA+OCT instrument (Heidelberg Engineering, Vista, CA, USA) using the eye-tracking

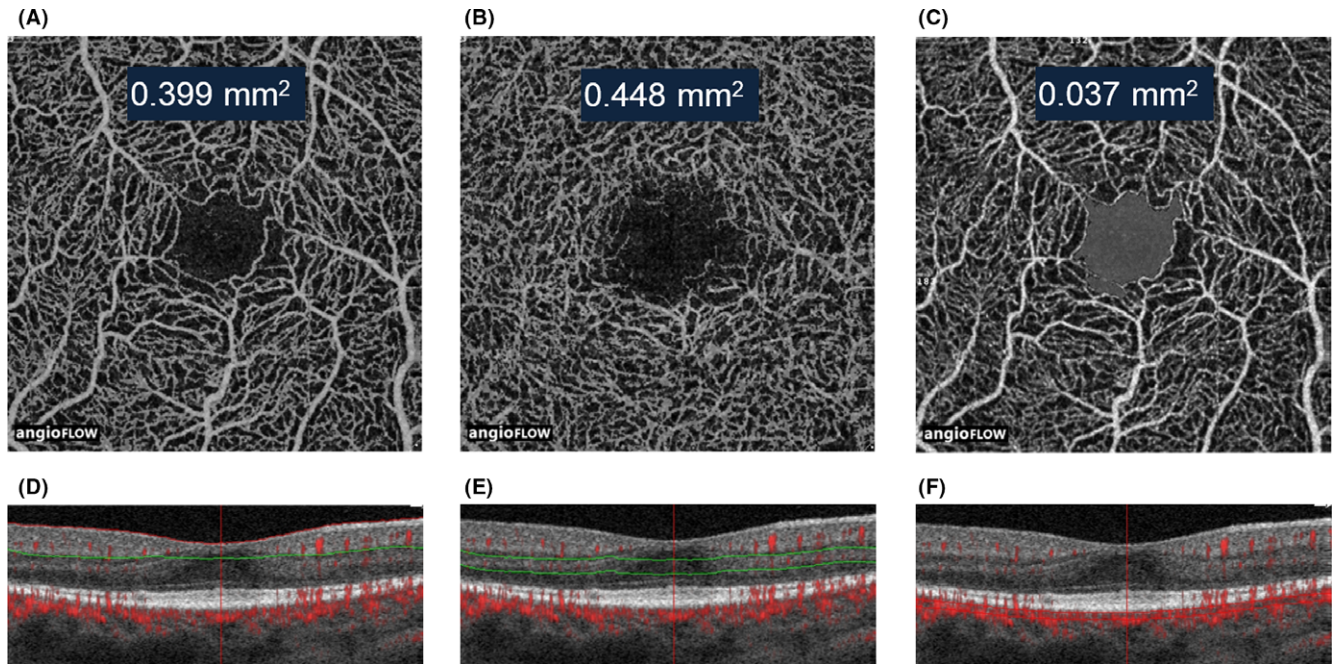


Fig. 1. The flow area in the superficial layer (A) and deep layer (B) as shown via optical coherence tomography angiography. The foveal avascular zone (C) was outlined manually. Each image was binarized and measured using the internal software of the instrument. The measurement range slab of each layer (superficial [D], deep [E] and choriocapillaris [F]).

feature. Nine-mm horizontal and vertical line scans through the fovea were obtained. The length of the inner segment ellipsoid (ISE) and the external limiting membrane (ELM) including the disrupted zone were measured manually by the distance measuring tools built into the OCT instrument. Then, the average of the horizontal and vertical ISE and ELM lengths was obtained.

Wide-field fundus autofluorescence

Wide-field fundus autofluorescence images were obtained with the Optos imaging system (Optos, Dunfermline, UK). To reduce the influence of peripheral image blurring, we cropped an elliptical area of 3000 × 2100 pixels from the original 3900 × 3072 pixel image for analysis. The areas without hypoa autofluorescence and hypera autofluorescence, abnormal FAF, were measured with IMAGEJ software (<http://imagej.nih.gov/ij/>; provided in the public domain by the National Institutes of Health, Bethesda, MD, USA). To reduce the influence of axial length, the areas were evaluated by the ratio between an elliptical area and the areas without abnormal FAF. In cases where the area without abnormal autofluorescence was separated, we

adopted only the area of island in the vicinity of the centre.

Visual field

Visual field testing was performed using the Goldmann perimeter procedure (Haag Streit, Bern, Germany). The results were scanned and analysed with IMAGEJ[®] software (<http://imagej.nih.gov/ij/>; provided in the public domain by the National Institutes of Health). The area of I-2e and I-4e on standard recording paper was measured under the system of calibration with a length of 212 pixels equivalent to 10.8 cm. The area was given in square centimetre (cm²) units.

Statistical analyses

Statistical analyses were performed using statistical software (SPSS[®], version 21.0; SPSS Science, Chicago, IL, USA). The results of descriptive analyses are reported as the mean ± standard deviation. A two-tailed Mann–Whitney *U*-test was used to compare retinal flow area of patients with RP and control subjects. Association between the individual parameters of OCTA and OCT parameters and FAF parameters were evaluated using mixed-effects regression analysis. All *p*-values <0.05 were

considered statistically significant. Intraclass correlation coefficient was calculated using the test–retest method with the 95% confidence interval (CI).

Results

Patients

We enrolled a total of 62 eyes from 62 patients, and 30 eyes were excluded because of poor image quality (*n* = 14), epiretinal membrane (*n* = 14) or cystoid macular oedema (*n* = 12). Fifty eyes from 32 patients with RP and 22 age- and refraction-matched normal eyes from 12 controls were included in the study. Table 1 shows the demographic data of patients with RP and normal controls. There was no statistically significant difference between the two groups in age (50.9 ± 10.7 versus 46.8 ± 12.6 years, respectively, *p* = 0.37, unpaired *t*-test), the ratio of men to women (3:11 versus 14:18, respectively, *p* = 0.089, chi-square test) and refraction dioptres (-0.43 ± 1.78 versus -0.45 ± 0.82 dioptres, respectively, *p* = 0.98, unpaired *t*-test).

We conducted genetic testing in fourteen patients and identified mutations in seven patients. The results showed *EYS* mutations in four patients, an *RDS* mutation in two

Table 1. Demographic data of patients with retinitis pigmentosa and normal controls.

	RP	Control	p-value
N	32	14	
Age (years)	46.8 ± 12.6	50.3 ± 10.0	0.33*
Sex (M:F)	14:18	3:11	0.089**
Refraction (dioptries)	-0.41 ± 1.32	0.05 ± 0.88	0.97*
log VA	0.11 ± 0.07	0.08 ± 0.05	0.69*

F = female; M = male; N = number; RP = retinitis pigmentosa; VA = visual acuity.

*Unpaired *t*-test.

**Chi-square test.

patients and *ROM1* mutations in one patient.

Clinical analyses

The flow area and FAZs in the normal and RP groups are shown in Fig. 3A–C. There were significant differences in the flow areas in the superficial (4.32 ± 0.27 mm² versus 3.99 ± 0.38 mm²; p = 0.007, Mann–Whitney *U*-test; Fig. 2A) and deep (4.44 ± 0.37 mm² versus 4.06 ± 0.71 mm²; p = 0.004, Mann–Whitney *U*-test; Fig. 2B) layers in normal and RP groups. However, there were no significant differences in the flow areas of the choriocapillaris layers (5.47 ± 0.13 mm² versus 5.43 ± 0.17 mm²; p = 0.353, Mann–Whitney *U*-test) in normal and RP groups (Fig. 2C).

Regarding FAZs, there were significant differences in the superficial layers (0.36 ± 0.07 mm² versus 0.30 ± 0.09 mm²; p = 0.006, Mann–Whitney *U*-test; Fig. 2D), but not in the deep layers (0.42 ± 0.09 mm² versus 0.41 ± 0.13 mm²; p = 0.237, Mann–Whitney *U*-test) in normal and RP groups (Fig. 2E).

Next, we investigated the association between OCTA parameters, the lengths of ISe and ELM on OCT images, the normal FAF area ratio and the areas of I-2 of the Goldmann perimeter in patients with RP (Table 2, Fig. 3). The flow area in superficial layers was significantly associated with the length of ISe ($Y = 9.275e^{-5}X + 3.543$, p = 0.001) and ELM ($Y = 9.595e^{-5}X + 3.476$, p = 0.002) and the areas of I-2e of the Goldmann perimeter

($Y = 0.018X + 4.018$, p = 0.036), but not with the normal FAF area ratio ($Y = 0.057X + 3.817$, p = 0.399) and the areas of I-4e of the Goldmann perimeter ($Y = 0.003X + 3.713$, p = 0.248).

The flow area in the deep layer did not show any significant association with the length of ISe ($Y = 8.097e^{-5}X + 3.608$, p = 0.185), ELM ($Y = 4.701e^{-5}X + 3.740$, p = 0.487), the normal FAF area ratio ($Y = 0.001X + 4.084$, p = 0.511) and the areas of I-2e ($Y = 0.031X + 3.891$, p = 0.502) and I-4e ($Y = 0.009X + 3.842$, p = 0.646) of the Goldmann perimeter. The ERG data of 70% of patients were nonrecordable.

The intraclass correlation coefficients in seven normal subjects for the flow areas in the superficial, deep and choriocapillaris layers were 0.91 (95% CI: 0.90–0.94), 0.90 (95% CI: 0.85–0.94) and 0.91 (95% CI: 0.89–0.93), respectively.

Discussion

We demonstrated the reduced flow area in the superficial vascular plexus in the macular area of patients with RP, which was associated with the lengths of ISe and ELM and

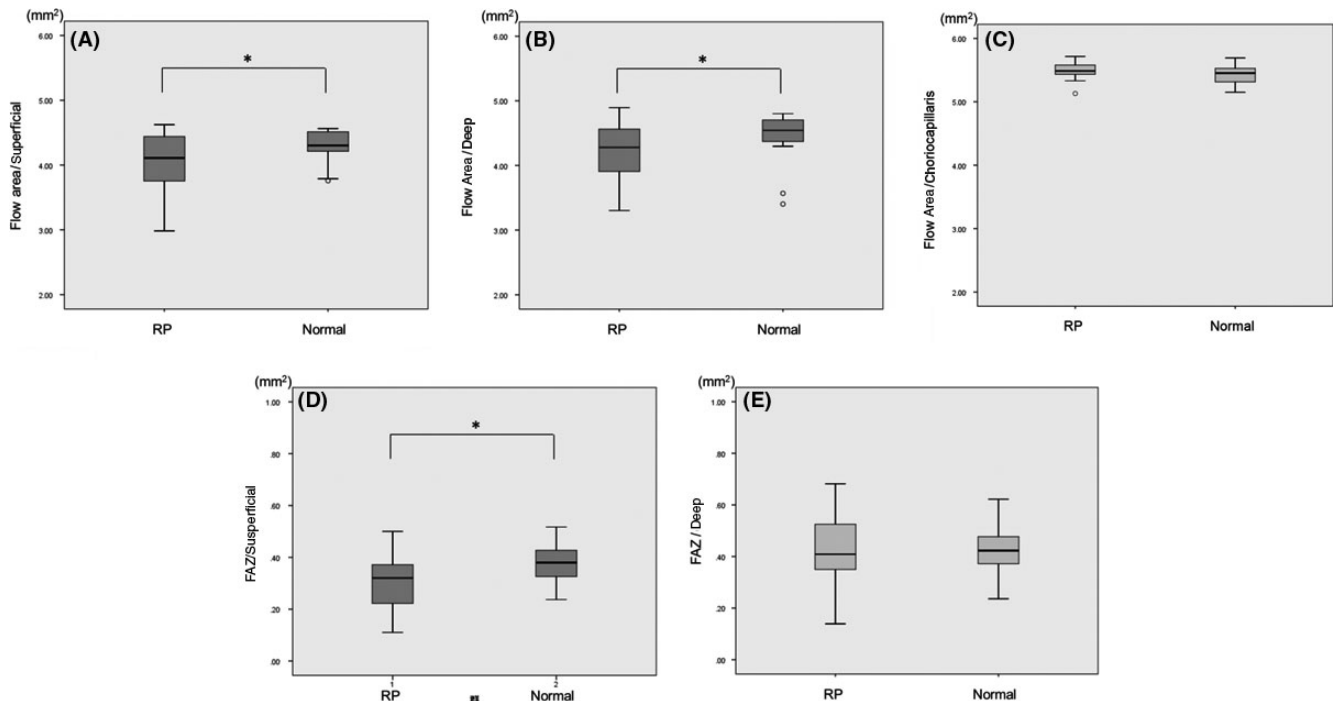


Fig. 2. The flow area in the superficial layer: (A), the deep layer (B) and the choriocapillaris (C) layer. There were significant differences between retinitis pigmentosa (RP) patients and normal subjects in the superficial and deep layers, but not in the choriocapillaris. The foveal avascular zone (FAZ) in the superficial (D) and deep layer (E). Data are also described as the mean ± standard error of the mean. *p < 0.05 using Mann–Whitney *U*-test. Box and whisker plots represent the median, upper and lower quartile, and the maximum and minimum values.

Table 2. Association between flow area in superficial layers and deep layers and the length of the inner ellipsoid segment (ISe) and external limiting membrane (ELM), the remaining normal area (NA) of fundus autofluorescence (FAF), and the area of I-2e and I-4e of the Goldmann perimeter (GP) studied using mixed-effects regression analysis.

		Flow area					
		Superficial			Deep		
		Regression coefficient	SE	p-Value	Regression coefficient	SE	p-Value
OCT	ISe	9.275×10^{-5}	2.490×10^{-5}	0.001	8.097×10^{-5}	2.490×10^{-5}	0.185
	ELM	9.595×10^{-5}	2.615×10^{-5}	0.002	4.701×10^{-5}	5.790×10^{-5}	0.487
FAF	NA	0.057	0.001	0.399	0.001	0.001	0.511
GP	I-2e	0.018	0.026	0.036	0.031	0.045	0.502
	I-4e	0.003	0.018	0.248	0.009	0.022	0.646

SE = standard error.

Goldmann I2e perimetric area. The flow area in the deep vascular plexus layers was also significantly smaller in patients with RP than in controls. However, OCTA flow in the deep vascular plexus layers did not show any significant association with other retinal findings of photoreceptor integrity or Goldmann perimetry.

Previous studies have demonstrated reduced retinal blood flow in patients with RP using several techniques, including high-resolution magnetic resonance imaging, laser speckle flowgraphy and laser Doppler flowmetry. Additionally, two recent studies have demonstrated decreased retinal blood flow density in patients with RP by OCTA: Parodi et al. (2017) demonstrated decreased flow density in the deep and superficial capillary plexus in patients with relatively early-stage RP (mean BCVA was 0.5 ± 0.3 LogMAR in 16 patients), and Rezaei et al. (2017) reported that microvascular changes in

the retinal and choroidal vasculature correlate with structural damage on OCTA images. These results correspond with the findings of the present study.

We included only the patients who had good VA ($\geq 20/20$); about 78% of patients exhibited remaining ISe > 3 mm (Fig. 3), and about 80% showed that the remaining I-4e area in Goldmann perimeter > 3 cm², which is the measurement range of OCTA. These results indicate that vascular impairment could exist even before morphological changes could be visualized on OCT images and functional changes in the perimeter could be detected. Makiyama et al. (2013) reported decreased cone density in eyes with RP, in spite of good VA and foveal sensitivity. Eysteinson et al. (2014) reported that decreased oxygen demand and increased venous saturation could trigger a decrease in retinal vessel diameter in patients with RP.

Another factor which may reduce vessel density in RP is increased endothelin-1 (ET-1) level, which is the most potent vasoconstrictor of vessels (Masaki et al. 1991). Cellini et al. found that plasma level of ET-1 was significantly increased in patients with RP compared to normal subjects. Taken together, these results indicate that the macular photoreceptors have not yet been lost (on OCT), but some have a reduction in function that was not detectable with measures of VA and Goldmann perimetry.

It is interesting to note that the association between flow area and the lengths of ISe and ELM was detected only in the superficial layers. This result is consistent with a recent OCTA study in patients with RP, in which there was no significant difference in foveal flow density in the deep layer between patients with RP and controls (Koyanagi et al. 2017). However, Koyanagi et al. also reported that parafoveal flow in the deep layers is significantly reduced in patients with RP. Further investigation of the range of retinal degeneration and blood flow reduction would be a step towards understanding the relationship between retinal blood flow and retinal photoreceptor degeneration.

The first sign of RP is the death of photoreceptors, followed by degeneration of bipolar and amacrine cells (Fariss et al. 2000) as well as Müller cells (Milam et al. 1998) present in the outer plexiform layer and INL. Therefore, we speculate that flow area and FAZ in the deep plexus layer, which is located more towards the periphery of

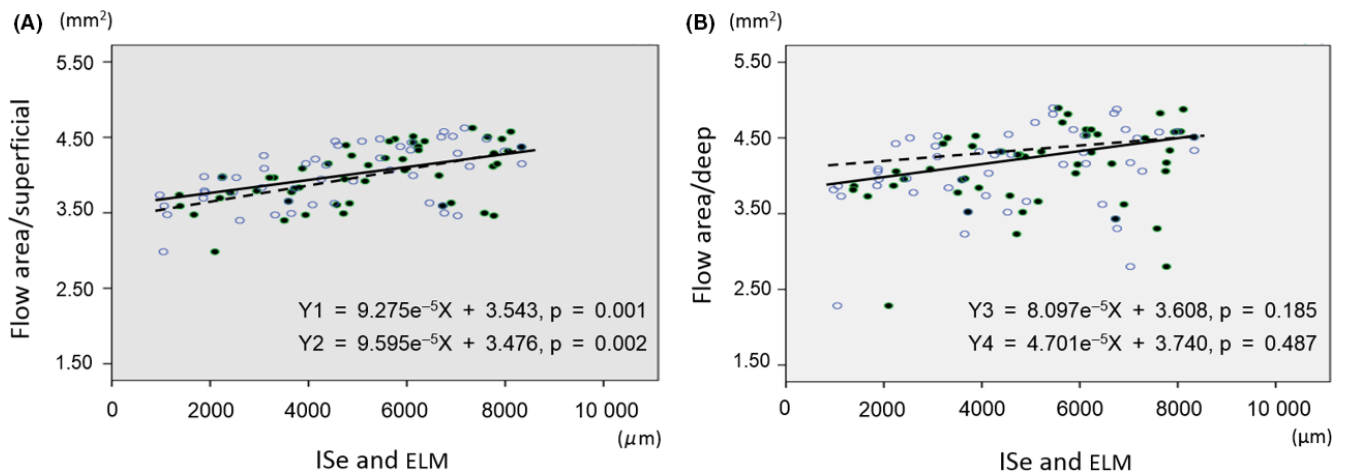


Fig. 3. The scatter plot of the flow areas in the superficial (A) and deep layers (B) and the lengths of the inner ellipsoid segment (ISe; white circle, Y1, and Y3) and external limiting membrane (ELM; black circle, Y2, and Y4). Solid and dashed lines represent the association between flow area and the length of ISe (solid line) and ELM (dashed line) using a linear mixed model with random effects.

the retina, are more sensitive to atrophy of the outer nuclear layer. However, the unexpected result of the present study is probably attributable to the remodelling of the inner retina. Huang et al. (2014) reported thickening of the INL on OCT images, attributed to retinal remodelling in patients with retinal degeneration due to *ABCA4* mutations. Additionally, Fernández-Sánchez et al. (2015) demonstrated high populations of astrocytes in the early phase of RP in a rat model. Moreover, remodelling of the inner retina has been reported in a mouse model of retinal degeneration (Kalloniatis et al. 2016). Müller cells exhibit metabolic alterations prior to obvious photoreceptor cell loss (Jones et al. 2016), and abnormal neuronal activity in postphotoreceptor neurons (amacrine cells, bipolar cells and ganglion cells) in the retinal inner layer has been well established (Stasheff et al. 2011). Increased demand for blood flow for regeneration or remodelling of the INL could cause blood flow redistribution in the deep layer plexus, which is located relatively close to the INL. With the OCTA technology, it is possible to separately analyse blood flow in the superficial and deep plexus *in vivo*, which could lead us to gain new insights on the circular alternation in disease progression.

The present findings also revealed a significant correlation between flow area and area of I-2 of the Goldmann perimeter. However, flow area and normal FAF area ratio were not significantly correlated. This is probably because the present study exclusively investigated the central area. The I-2 area of the Goldmann perimeter represents central vision sensitivity, while the normal FAF area ratio represents a relatively large area of remaining vision. About 86% of the patients had a remaining FAF area $>3 \text{ cm}^2$. In contrast, about 30% of the patients showed that the remaining I-2e area in Goldmann perimeter was $>3 \text{ cm}^2$. The areas with isoautofluorescence and hyperautofluorescence were reported to correlate well with the areas of the VF on Goldmann perimetry (Ogura et al. 2014). Several previous studies have reported similar correlations between circulatory parameters and central visual function. Decreased macular blood flow measured by the laser speckle technique has been shown to be

correlated with reduced macular visual sensitivity measured using the Humphrey visual field test (Murakami et al. 2015). Moreover, foveal deep vessel density measured using OCTA has been reported to be correlated with multifocal electroretinogram findings (Toto et al. 2016). Taken together, these results suggest that decreased blood flow in the central area is involved in pathogenesis of RP in the macular area.

The present findings demonstrated no differences in the choriocapillaris plexus layer between patients with RP and normal subjects. Several studies have reported altered choroid circulation in patients with RP (Falsini et al. 2011). However, there is a lack of agreement on the findings of flow area in the choriocapillaris between two previous studies: while Parodi et al. reported no differences in choriocapillaris capillary plexus density between patients with relatively early-stage RP and control subjects, Toto et al. reported that choriocapillaris capillary plexus densities in patients with middle- and late-stage RP were significantly lower compared to those in control subjects. This reduction in choriocapillaris capillary plexus density is probably secondary to the stage of RP. A previous study has demonstrated the choriocapillaris to be missing from retinal regions that have lost photoreceptors and formed bone spicule pigment (Li et al. 1985). However, it is not known whether the choriocapillaris is altered in the very early stages of RP, when the RPE is almost intact. Longitudinal, rather than cross-sectional, studies beginning from the early phase of the disease would help resolve this question.

We found that the FAZ area was significant smaller in patients with RP than in controls in the superficial layers but not in the deep layers. Recent studies are not conclusive regarding the expansion of the FAZ in patients with RP. Parodi et al. (2017) reported that the FAZ at the deep capillary plexus level was larger in patients with RP than in controls. On the other hand, Koyanagi et al. (2017) found no significant difference in the FAZ in both superficial and deep layers between patients with RP and controls. One possible reason for this discrepancy is that we included only patients with good VA, meaning that foveal function was almost intact. A time-course study is necessary to investigate

the change in FAZ during progression to advanced disease.

As mentioned above, recent blood flow measurement techniques included the laser Doppler method and laser speckle flowgraphy (Pournaras & Riva 2013). Regarding their respective properties, the true rate of blood flow in retinal vessels can be more accurately determined using the laser Doppler method (Yoshida et al. 2003). However, comparatively more time is needed to calculate the measurements; therefore, subject compliance varies widely. Laser speckle flowgraphy can measure the amount of retinal vessel blood flow in a comparatively short time. However, some of the resulting parameters, such as the value of the normalized blur, are relative and not suitable for comparisons between subjects (Sugiyama 2014). In contrast, OCTA shows the area of vessels containing the blood flow with a frame speed (lesser and more than a certain speed), as a flow area with a split-spectrum amplitude-decorrelation angiography (SSADA) algorithm. Using this algorithm, two consecutive OCT B-scans were compared to calculate the decorrelation in the images (Jia et al. 2012). On the analysis screen of the Optovue, blood vessels were reconstructed to appear in two dimensions when viewed from the top (Fig. 1). Furthermore, the image was binarized and the area of the section which contained the signals was determined as the flow area. OCTA has the advantages of being fast, noninvasive, and can provide highly quantitative data. A strong point of OCTA is its utility in general examinations compared with that of circular examination instruments, because OCTA uses existing OCT images, is widely adaptable and is clinically used worldwide. Therefore, OCTA imaging could be very useful in daily clinical diagnoses or for long-term follow-up. However, if the speed of blood flow is not constant, the blood vessel cannot be visualized; in such a case, whether the true area of the blood vessel is presented will be unclear (Spaide et al. 2015). Moreover, information regarding the relationship between the flow areas determined using OCTA and the information from other procedures that show the true blood flow, such as laser Doppler methodology, are insufficient. Additional blood flow measurement devices have recently become available, making it possible to understand the

advantages and disadvantages of each device; this is desirable for a comprehensive assessment of multimodal imaging techniques.

A limitation of our study was the small number of cases and lack of information regarding genotype and mode of inheritance in spite of PR being a heterogeneous disease. Different gene mutations may cause a variety of pathological phenotypes, including vascular defect. Future studies should explore whether different genotypes have varying patterns of OCTA loss. Due to the reproducibility limitations of the OCTA examination, we examined only normal subjects because RP patients without any complication visited at 6-month or 1-year intervals, which was insufficient to ensure reproducibility. Therefore, the values from the normal subjects were measured repeatedly and may be a better estimate of their 'true' values than those of patients with RP. Our data may not coincide with the patients of less than -6 and greater than +3 dioptres because of exclusion criteria, further investigation of the relationships between refraction, axial length and flow area using OCTA are needed.

We found that the flow area determined using OCTA correlates with residual function determined using the Goldmann perimeter area and residual structural parameter measured using OCT. Further studies regarding blood flow could contribute to the understanding of pathogenesis of RP and may lead to improved photoreceptor rescue in RP.

References

- Berson EL (1993): Retinitis pigmentosa. The Friedenwald Lecture. *Invest Ophthalmol Vis Sci* **34**: 1659–1676.
- Daiger S, Sullivan L & Bowne S (2013): Genes and mutations causing retinitis pigmentosa. *Clin Genet* **84**: 132–141.
- Eysteinnsson T, Hardarson SH, Bragason D & Stefánsson E (2014): Retinal vessel oxygen saturation and vessel diameter in retinitis pigmentosa. *Acta Ophthalmol* **92**: 449–453.
- Falsini B, Anselmi G, Marangoni D, D'F, Fadda A, Di Renzo A, Campos EC & Riva CE (2011): Subfoveal choroidal blood flow and central retinal function in retinitis pigmentosa. *Invest Ophthalmol Vis Sci* **52**: 1064–1069.
- Fariss RN, Li ZY & Milam AH (2000): Abnormalities in rod photoreceptors, amacrine cells, and horizontal cells in human retinas with retinitis pigmentosa. *Am J Ophthalmol* **129**: 215–223.
- Fernández-Sánchez L, Lax P, Campello L, Pinilla I & Cuenca N (2015): Astrocytes and Müller cell alterations during retinal degeneration in a transgenic rat model of retinitis pigmentosa. *Front Cell Neurosci* **22**: 484.
- Grunwald J, Maguire A & Dupont J (1996): Retinal hemodynamics in retinitis pigmentosa. *Am J Ophthalmol* **122**: 502–508.
- Hartong D, Berson E & Dryja T (2006): Retinitis pigmentosa. *Lancet* **368**: 1795–1809.
- den Hollander A, Black A, Bennett J & Cremers F (2010): Lighting a candle in the dark: advances in genetics and gene therapy of recessive retinal dystrophies. *J Clin Invest* **120**: 3042–3053.
- Huang WC, Cideciyan AV, Roman AJ, Sumaroka A, Sheplock R, Schwartz SB, Stone EM & Jacobson SG (2014): Inner and outer retinal changes in retinal degenerations associated with ABCA4 mutations. *Invest Ophthalmol Vis Sci* **55**: 1810–1822.
- Iacono P, Parodi MB, Bandello F, La Spina C & Zerbini G (2017): Dynamic and static vessel analysis in patients with retinitis pigmentosa: a pilot study of vascular diameters and functionality. *Retina* **37**: 998–1002.
- Jia Y, Tan O, Tokayer J et al. (2012): Split-spectrum amplitude-decorrelation angiography with optical coherence tomography. *Opt Express* **20**: 471047–471125.
- Jones BW, Pfeiffer RL, Ferrell WD, Watt CB, Marmor M & Marc RE (2016): Retinal remodeling in human retinitis pigmentosa. *Exp Eye Res* **150**: 149–165.
- Kalloniatis M, Nivison-Smith L, Chua J, Acosta ML & Fletcher EL (2016): Using the rd1 mouse to understand functional and anatomical retinal remodeling and treatment implications in retinitis pigmentosa: a review. *Exp Eye Res* **150**: 106–121.
- Koyanagi Y, Murakami Y, Funatsu J et al. (2017): Optical coherence tomography angiography of the macular microvasculature changes in retinitis pigmentosa. *Acta Ophthalmol* [Epub ahead of print].
- Li Z, Possin D & Milam A (1985): Histopathology of bone spicule pigmentation in retinitis pigmentosa. *Ophthalmology* **102**: 805–816.
- Ma Y, Kawasaki R, Dobson LP, Ruddle JB, Kearns LS, Wong TY & Mackey DA (2012): Quantitative analysis of retinal vessel attenuation in eyes with retinitis pigmentosa. *Invest Ophthalmol Vis Sci* **53**: 4306–4314.
- Makiyama Y, Ooto S, Yoshimura N et al. (2013): Macular cone abnormalities in retinitis pigmentosa with preserved central vision using adaptive optics scanning laser ophthalmoscopy. *PLoS ONE* **19**: e79447.
- Masaki T, Kimura S, Yanagisawa M & Goto K (1991): Molecular and cellular mechanism of endothelin regulation implication for vascular function. *Circulation* **84**: 1457–1468.
- Milam A, Zong Y & Fariss R (1998): Histopathology of the human retina in retinitis pigmentosa. *Prog Retin Eye Res* **17**: 175–205.
- Murakami Y, Ikeda Y, Akiyama M et al. (2015): Correlation between macular blood flow and central visual sensitivity in retinitis pigmentosa. *Acta Ophthalmol* **93**: 644–648.
- Ogura S, Yasukawa T, Kato A, Usui H, Hirano Y, Yoshida M & Ogura Y (2014): Wide-field fundus autofluorescence imaging to evaluate retinal function in patients with retinitis pigmentosa. *Am J Ophthalmol* **158**: 1093–1098.
- Parodi MB, Cicinelli MV, Rabiolo A, Pierro L, Gagliardi M, Bolognesi G & Bandello F (2017): Vessel density analysis in patients with retinitis pigmentosa by means of optical coherence tomography angiography. *Br J Ophthalmol* **1**–5.
- Pournaras CJ & Riva CE (2013): Retinal blood flow evaluation. *Ophthalmologica* **229**: 61–74.
- Rezaei KA, Zhang Q, Chen CL, Chao J & Wang RK (2017): Retinal and choroidal vascular features in patients with retinitis pigmentosa imaged by OCT based microangiography. *Graefes Arch Clin Exp Ophthalmol* **255**: 1287–1295.
- Spaide R, Fujimoto J & Waheed N (2015): Optical coherence tomography angiography. *Retina* **35**: 2161–2162.
- Stasheff SF, Shankar M & Andrews MP (2011): Developmental time course distinguishes changes in spontaneous and light-evoked retinal ganglion cell activity in rd1 and rd10 mice. *J Neurophysiol* **105**: 3002–3009.
- Sugiyama T (2014): Basic technology and clinical applications of the updated model of laser speckle flowgraphy to ocular diseases. *Photonics* **1**: 220–234.
- Toto L, Borrelli E, Mastropasqua R, Senatore A, Di Antonio L, Di Nicola M, Carpineto P & Mastropasqua L (2016): Macular features in retinitis pigmentosa: correlations among ganglion cell complex thickness, capillary density, and macular function. *Invest Ophthalmol Vis Sci* **57**: 6360–6366.
- Yoshida A, Feke GT, Mori F, Nagaoka T, Fujio N, Ogasawara H, Konno S & McMell J (2003): Reproducibility and clinical application of a newly developed stabilized retinal laser Doppler instrument. *Am J Ophthalmol* **135**: 356–361.
- Yu DY & Cringle SJ (2005): Retinal degeneration and local oxygen metabolism. *Exp Eye Res* **80**: 745–751.

Received on January 10th, 2017.
Accepted on November 21st, 2017.

Correspondence:

Yasuhiko Hirami, MD, PhD
Department of Translational Research
Division of Ophthalmology
Institute of Biomedical Research and
Innovation
2-2, Minatojima-Minamimachi, Chuo-ku
Kobe 650-0047
Japan
Tel: +81 78 306 0111
Fax: +81 78 306 0101
Email: hirami@fbri.org